



**Manchester  
Metropolitan  
University**

---

Crapnell, Robert D and Banks, Craig E (2022) Electroanalytical overview: the determination of manganese. *Sensors and Actuators Reports*, 4. p. 100110. ISSN 2666-0539

---

**Downloaded from:** <https://e-space.mmu.ac.uk/630837/>

**Version:** Published Version

**Publisher:** Elsevier

**DOI:** <https://doi.org/10.1016/j.snr.2022.100110>

**Usage rights:** Creative Commons: Attribution-Noncommercial-No Derivative Works 4.0

Please cite the published version

<https://e-space.mmu.ac.uk>



## Electroanalytical overview: The determination of manganese

Robert D. Crapnell, Craig E. Banks\*

Faculty of Science and Engineering, Manchester Metropolitan University, Chester Street, Manchester M1 5GD, United Kingdom

### ARTICLE INFO

**Keywords:**  
Manganese (II)  
Electrochemistry  
Electroanalytical  
Sensor  
Electrode

### ABSTRACT

Manganese is an essential nutrient of the human body but also toxic at elevated levels with symptoms of neurotoxicity reported, therefore its analytical determination is required. Manganese (II) is ingested primarily through food and drinking water so its routine monitoring in such samples is essential. While laboratory based analytical instrumentation can be routinely used to measure manganese (II), there is a need to develop methods for manganese (II) determination that can be performed in-the-field utilizing simple and inexpensive instrumentation yet providing comparable sensitive analytical measurements. Electrochemistry can provide a solution with instrumentation readily portable and hand-held coupled with electrochemical sensing platforms that are sensitive and provide on-site rapid analytical measurements. Consequently, in this overview we explore the electroanalytical determination of manganese (II) reported throughout the literature and offer insights into future research opportunities within this important field.

### 1. Introduction: manganese

Manganese is an essential element for humans and is necessary for the formation of arginase and glutamine synthetase while superoxide dismutase, an important antioxidant mitochondrial enzyme, also requires manganese for its formation [1]. While being an essential nutrient, at elevated levels it is a health concern and can show symptoms of neurotoxicity with manganese exposure in children reported to cause adverse neurodevelopmental outcomes [2,3]. Chronic exposure to manganese is termed *Manganism* which was first described by John Couper in 1837 when two workers in Scotland involved in the grinding of manganese ore developed paraplegia [1]. *Manganism* has been reported to most often be observed in the mining, smelting, and grinding of manganese. Manganese can exist in 11 oxidation states but the most environmentally and biologically important manganese compounds are those that contain  $Mn^{2+}$ ,  $Mn^{4+}$  or  $Mn^{+7}$ . Manganese occurs naturally in many surface waters and groundwater sources, and in soils that erode into these waters. However, human activities are also responsible for a large amount of the manganese contamination in water in some areas. Ingestion through food and drinking water are the main routes of manganese exposure for the general population. The United States Environmental Protection Agency (US EPA) has established National Secondary Drinking Water Regulations that set non-mandatory water quality standards (secondary maximum contaminant levels or SMCLs) that are used as guidelines to assist water systems with managing

drinking water for aesthetic considerations, such as taste, color, and odour. The EPA has set a SMCL for manganese (II), total dissolved of 5 mg/L (5 ppb, ~91 nM) in order to protect against black staining and bitter metallic-tasting water. Frisbie and co-workers [4] have reported that drinking-water supplies with Mn concentrations > 400 µg/L are found in a 54 countries worldwide affecting many tens of millions of people. As a result, manganese is required to be analytically measured.

Manganese (II) can be determined by standard laboratory techniques such as atomic absorption spectrometry [5,6], fluorimetry [7], x-ray fluorescence [8], and inductively coupled plasma atomic emission spectroscopy [9,10]. There is a need to develop methods of manganese (II) determination that use simple and inexpensive instrumentation but that gives accurate and sensitive analytical results and allows for measurements to be taken in-the-field. Electrochemical methods provide a solution to this with potentiostats now being hand-held and battery operated coupled with electrodes that have many advantages such as high sensitivity, low cost, rapid analysis time and portability [11]. In this review, the recent advances in the electroanalytical sensing of manganese (II) are overviewed with future challenges and opportunities also highlighted.

#### 1.1. Electroanalytical approaches

Table 1 presents the recent approaches reported for the electroanalytical detection of manganese (II). We will consider key highlights

\* Corresponding author.

E-mail address: [c.banks@mmu.ac.uk](mailto:c.banks@mmu.ac.uk) (C.E. Banks).

**Table 1**

An overview of various electrochemical approaches reported for the detection of manganese. Highlighting the electrode used with any modifications, the electro-analytical method used and deposition time, the key analytical parameters of linear range and limit of detection alongside the real sample medium tested in (if applicable).

Electrode	Method of Detection	Linear Range	Deposition time	Limit of Detection	Sample Medium	Ref.
Graphite	DP-CSV	0.4–60 $\mu\text{g L}^{-1}$	6 min	3 $\mu\text{g L}^{-1}$	Mineral waters	[29]
Bromopyrogallol - HMDE	ASV	$6 \times 10^{-10}$ – $1.5 \times 10^{-7}$ M	3 min	$4 \times 10^{-10}$ M	–	[35]
Graphite	DP-CSV	Down to 4 ppb	300 s	–	Ground and river water	[28]
GC-RDE	DPV-CSV	–	10 min	6 nM	Coastal and estuarine waters	[68]
1-(2-pyridylazo)–2-naphthol - CPE	DP-CSV	$1.0 \times 10^{-8}$ – $1.0 \times 10^{-7}$ M, $1.0 \times 10^{-7}$ – $1.0 \times 10^{-5}$ M	200 s	$6.9 \times 10^{-9}$ M	Seawater	[36]
GC	SW-CSV	0.005 – 2.0 $\mu\text{M}$	180 s	–	Cement	[31]
BDD	DP-CSV	$10^{-11}$ – $3 \times 10^{-7}$ M	2 min	$10^{-11}$ M	Instant tea	[39]
Hg	DP-ASV	–	240 s	$1.73 \times 10^{-10}$ M	Reference materials of seawater, lagarosiphon major and cod muscle	[69]
GC	SW-CSV	$1.0 \times 10^{-9}$ – $4 \times 10^{-8}$ M	120 s	$2.5 \times 10^{-10}$ M	–	[43]
Graphite/styrene-acrylonitrile copolymer composite electrode	SW-CSV	0.2–10 $\mu\text{g L}^{-1}$	180 s	0.2 $\mu\text{g L}^{-1}$	–	[70]
HMDE	DPASV	–	4 min	2.5 $\mu\text{g L}^{-1}$	Ground and tap water	[16]
GC	LSV	$4 \times 10^{-8}$ – $1 \times 10^{-6}$ M	–	–	River and lake water, raw sugar	[30]
Carbon film	SW-CSV	–	120 s	3.9 nM	Sediment samples	[18]
BDD	DP-CSV	1.25–25 $\mu\text{M}$	60 s	$7.4 \times 10^{-7}$ M	Marine sediments	[47]
EPPG	DP-CSV	0.62–17.4 $\mu\text{M}$	30 s	0.29 $\mu\text{M}$	–	[49]
BDD	DP-CSV	$4 \times 10^{-8}$ – $17.3 \times 10^{-8}$ M	120 s	$8.9 \times 10^{-9}$ M	Seawater	[71]
Formazan modified GC	AdSV-CSV	0.1–30 $\mu\text{g L}^{-1}$	60 s	0.04 $\mu\text{g L}^{-1}$	Spring, tap, mineral and seawater	[33]
EPPG	DP-CSV	25–250 nM	120 s	14.2 nM	Certified seawater sample	[48]
BDD-MEA	SW-CSV	1.8–9.2 $\mu\text{M}$	120 s	49 nM	–	[44]
ISE	potentiometric	$5.0 \times 10^{-6}$ – $1.0 \times 10^{-1}$ M	–	–	Multi-vitamin tablet and wastewater	[54]
Mercury film - Ag	DP-ASV	–	120 s	0.3 nM	rainwater	[17]
Bentonite–porphyrin CPE	ASV	$6 \times 10^{-7}$ – $5 \times 10^{-4}$ M	4 min	$1.07 \times 10^{-7}$ M	Wheat flour, rice and vegetables	[72]
SPE	SW-CSV	90–1780 nM	30 s	64 nM	–	[62]
ISE	potentiometric	$1.0 \times 10^{-5}$ – $1.0 \times 10^{-1}$ M	–	$8.0 \times 10^{-6}$ M	Tablets and syrup	[55]
Gold electrode	ASC	1.5–12 nM	300 s	1.4 nM	Seawater	[45]
SPE	SW-CSV	73–504 nM	120 s	63 nM	–	[61]
CNTS	SW-CSV	0.6–6.7 $\mu\text{M}$	60 s	93 nM	Pond water	[20]
Pd	SW-CSV	455 nM–10.9 $\mu\text{M}$	600 s	334 nM	Pond water	[26]
Pyrolytic graphite	potentiometric	$1.23 \times 10^{-8}$ – $1.0 \times 10^{-1}$ M	–	$4.78 \times 10^{-9}$ M	Wastewater, soil and vegetables	[51]
Pt	SW-CSV	91–910 nM	900 s	16.3 nM	Pond water	[27]
Au	SW-CSV	$1.1$ – $2.0 \times 10^{-7}$ M, $2.0$ – $3.2 \times 10^{-7}$ M	180 s	$3.1 \times 10^{-8}$ M	Cement and clinker samples	[25]
Additive Manufactured Electrode	DP-CSV	$9.1 \times 10^{-9}$ – $2.7 \times 10^{-6}$ M	350 s	$1.6 \times 10^{-9}$ M	Drinking water and certified drinking water sample	[65]
GC	DP-CSV	2.5–200 $\mu\text{g L}^{-1}$	240 s	0.63 $\mu\text{g L}^{-1}$	Tap and lake water	[32]
GC	DPV-CSV	1–7 $\mu\text{M}$	300 s	0.43 $\mu\text{M}$	–	[34]
Pt	SW-CSV	91 nM–1.82 $\mu\text{M}$	–	10.1 nM	Drinking water	[63]

(continued on next page)

Table 1 (continued)

Electrode	Method of Detection	Linear Range	Deposition time	Limit of Detection	Sample Medium	Ref.
SPE / Au NPs / rGO/Fe <sub>3</sub> O <sub>4</sub> NPs / L-cysteine	SW-CSV	0.5–300 µg L <sup>-1</sup> , 62–1500 µg L <sup>-1</sup>	900 s 300, 30 s, respectively	34, 1500 µg L <sup>-1</sup> , respectively	Soil samples	[64]

**Key:** SPEs: screen-printed electrodes; GC: glassy carbon; BDD: boron-doped diamond; Au NPs : gold nanoparticles; rGO; reduced graphene oxide; CPE: carbon paste electrode; RDE: rotating disc electrode; EPPG: edge plane pyrolytic graphite electrode; ASC: anodic stripping chronoamperometry; BDD-MEA: boron-doped diamond microelectrode array; AdSV: adsorptive stripping voltammetry; HMDE: hanging mercury drop electrode; SW: square wave voltammetry; CSV: cathodic stripping voltammetry; DP/V: differential pulse voltammetry; CNTs: carbon nanotubes; ISE: ion-selective electrode.

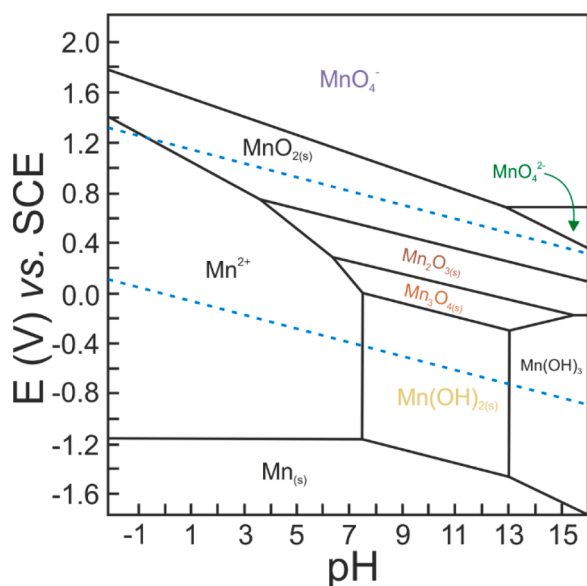


**Fig. 1.** Pourbaix diagram showing the possible thermodynamically stable phases of manganese. The boundaries representing the 50/50% presence of states is represented by solid lines and the stability of water in the system is represented by dashed lines.

below. Manganese (II) can be determined electrochemically at mercury film electrodes [12,13], dropping mercury electrodes [14–16] and renewable mercury film silver based electrodes, for example, via anodic stripping voltammetry (ASV) [17]. Eq. (1) describes the pre-concentration step for the electrochemical/electroanalytical determination of manganese (II). Following the application of a suitably negative applied potential for a set-time, manganese (II) is accumulated upon the electrode surface in the form of manganese metal:



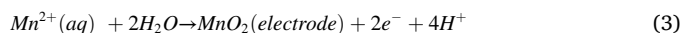
The Pourbaix diagram for manganese is presented in Fig. 1, which shows the electrochemical stability for different redox states of manganese as a function of pH. The potential is then swept positively to induce Faradaic loss of the accumulated manganese metal, as described by:



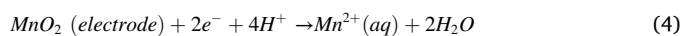
This is shown within Scheme 1, which provides an overview of this process where following Eq. (2) a characteristic peak, so called a “stripping peak” due to manganese metal being “stripped” from the electrode surface is observed; the peak height and / or peak area can be used to provide quantification of the manganese ion. In the early years of electrochemical development, mercury was the first port-of-call, but use of mercury suffers from three key issues [18]: (i) the low solubility of manganese (II) in mercury, (ii) the deposition potential for manganese

(II) by reduction which is close to the hydrogen ion reduction potential, and (iii) the formation of intermetallic compounds. As a result, this limits the sensitivity of the electroanalytical approach. Furthermore, given the environmental issues around mercury and its ban in some countries, researchers have moved to other electrode materials and approaches. While anodic stripping voltammetry at electrodes, other than mercury may be utilized, such as silver amalgam electrodes [19], and solid electrodes, the anodic stripping voltammetry of manganese is more difficult due to the highly negative potential for the electrochemical process to occur, see Eq. (1).

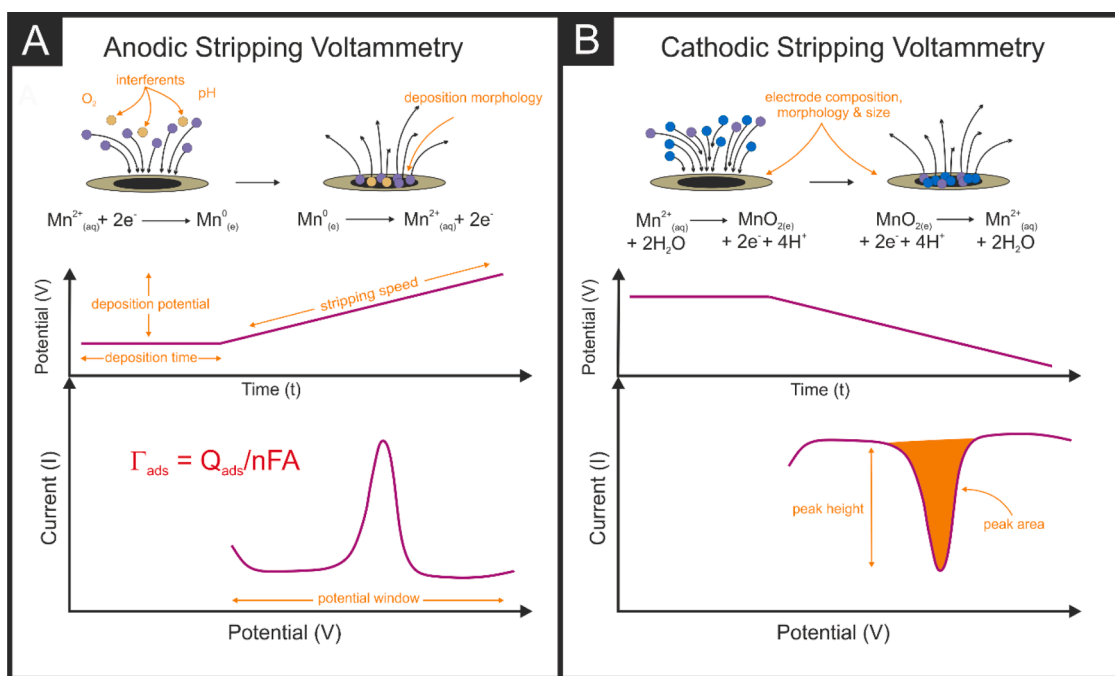
A notable alternative approach is the use of cathodic stripping voltammetry (CSV) where, in this approach, manganese (II) is electro-deposited upon a chosen electrode surface from the application of a suitable positive potential forming a manganese (IV) dioxide film:



The current is then swept negatively, revealing a stripping signal where the peak current and area of the stripping signal provides the analytical peak to quantify manganese:



Where again, a characteristic stripping peak will be observed allowing quantification of manganese; Scheme 1 shows an overview. The method can be optimised through vigilant choice of the electrode surface and composition, and the electrochemical parameters (deposition time, applied potential etc.). To compare and contrast the two approaches of anodic and cathodic stripping voltammetry, Yue et al. [20] compared the anodic and cathodic detection of manganese (II) at a catalyst free carbon nanotube electrode – note that metallic impurities within carbon nanotubes which are used for their fabrication via chemical vapour deposition can remain and dominate the electrochemical response [21,22]. That said, significant advances have been made to produce metallic free carbon nanotubes such as being synthesised using a carbon thermal carbide conversion method [20]. Returning to the work of Yue et al., the authors found that detection limits for 120 nM and 93 nM were achieved for anodic and cathodic stripping voltammetry, respectively, using a deposition time of 60 s; a narrow linear range of detection and poor stripping peak shape was observed in the case of anodic stripping voltammetry where in contrast, the cathodic stripping voltammetry was found to have a better analytical sensitivity and was robust enough to utilize for the determination of manganese in pond water. Another issue are interferences, in the case of ASV, most, if not all metal ions will electrochemically deposit when high enough overpotentials are applied. In the case of CSV, only certain metal ions are able to undergo this process within a suitable timeframe, which on one hand limits its widespread use, but on the other, makes it more selective (see later for more details). Additionally, CSV is also free from interference by intermetallic species, a side-effect which often plagues ASV, where overlapping peaks can be observed. The above gives clear arguments to adopt the cathodic stripping voltammetry of manganese, and from inspection of Table 1, it is clear that researchers have adopted this.



**Scheme 1.** Cartoon showing the process occurring above the general equations, waveshape applied and an example output for both anodic stripping voltammetry (A) and cathodic stripping voltammetry (B). Labels in orange denote key parameters the researcher should consider when performing stripping voltammetry experiments along with the key outputs.

Returning to the cathodic stripping voltammetry mechanism, a more detailed mechanism has been suggested on platinum electrodes in acidic solutions [23]:



Nijjer and co-workers [24] have reported that the mechanism occurs via Eqs. (5)–(10) in acidic solutions using a platinum electrode followed by:



There are select reports utilizing metallic electrodes such as gold [25], Pd [26] and Pt [27] which exhibit linear ranges in the micro-molar concentration range, but it appears their use is rather limited for the sensing of manganese (II). Graphite electrodes [28,29] with detection limits in the range  $10^{-8}$  M have been reported and glassy carbon, a favourite electrode material of the electrochemist has been utilized for the sensing of manganese (II), either unmodified or modified [30–34]. In the latter case, a ligand is either put into the electrolyte or upon the chosen electrode surface to reduce the detection limit for manganese (II) and enhance the reversibility of its electrochemical system. Such an approach is known as adsorptive stripping voltammetry (AdSV). For example, the ligand formazan was surface modified upon a glassy carbon electrode which was able to measure manganese (II) from 0.1 to 30  $\mu\text{g L}^{-1}$  using a 60 s deposition time and AdSV-CSV, producing a limit of

detection (LOD) of 0.04  $\mu\text{g L}^{-1}$ , which was then used to measure manganese (II) in spring, tap, mineral and seawater samples [33]. Other approaches have utilized bromopyrogallol red [35], 1-(2-pyridylazo)-2-naphthol [36], and diethylenetriaminepentaacetic acid [37] for example. Other electrodes have been explored towards the detection of manganese (II), such as carbon nanotubes [20] and carbon film electrodes fabricated from carbon resistors [18], which allowed low nM sensing of manganese (II) and was applied to its measurement in sediment samples, which agreed well with independent ICP-AAS analysis.

The use of boron-doped diamond (BDD) as an electrode substrate is now well established in the field of electrochemistry, particularly electroanalysis and stripping voltammetry due to its accepted benefits which include: a wide potential window (3.5–4.0 V in aqueous media), low background currents, high resistance to electrode fouling, ease of chemical modification, long term stability, low sensitivity to dissolved oxygen and the hard and flat nature of the electrode surface [38]. Saterlay and co-workers [39] have used the synergy of power ultrasound (20 kHz) with BDD for the determination of manganese (II). In this approach, they utilize the well-known benefits of applying ultrasound into electroanalytical processes during the preconcentration step, then terminated when the potential is swept to quantify the analytical target [40,41]. The application of ultrasound results in acoustic streaming providing a strong convective flow of the target analyte to the electrode surface and at insonation powers about the cavitation threshold, bubble formation on the electrode surface provides an in-situ cleaning mechanism, which removes possible passivating materials found in real samples. This *in-situ* mechanism may involve oscillation bubbler and / or microjetting providing a strong shear flow across the electrode surface [42]. Saterlay et al. [39] successfully utilized power ultrasound, utilizing both benefits of power ultrasound coupled with BDD for the ultra-low level sensing of manganese (II) with a linear range from  $10^{-11}$  to  $3 \times 10^{-7}$  M, possible with a detection limit of  $10^{-11}$  M using a 2 min deposition time. In terms of potential interferences, in the case of ASV, if the sample contains multiple metal ion species, applying a suitability high overpotential will result in their electrodeposition, where competition for nucleation sites will occur upon the electrode surface, thus limiting the analytical sensitivity. However, in the case of CSV, only



certain metal ions are able to undergo this process within the timeframes of the experiment. To exemplify this, Saterlay et al. [39] tested their sonoelectroanalytical methodology towards the potential interferents of lead, copper, iron, zinc, mercury and aluminium ions. Zinc, copper, lead and iron (III) ions were found to have no measurable impact upon the technique's response to manganese (II), even when present at concentrations exceeding 100-fold that of manganese (II). The presence of mercury ions in solution at levels at least 50-fold those of manganese (II) also had no effect and the technique was also tolerant to nearly a fivefold excess over manganese of aluminium ions. Clearly this demonstrates why researchers adopt CSV for the determination of manganese (II). Last, Saterlay et al. [39] demonstrated successfully that the protocol can be used to measure manganese in instant tea samples, giving excellent agreement with independent AAS analysis. Similar work has recently been reported [43]. As is well known in electrochemistry, mass transport benefits can be realised through intelligent design of the electrodes. Usually, BDD electrodes can be fabricated as both macro- and micro-electrodes where the latter has significant advantages over the former with differences in the voltammetric signature evident. For the case of a macroelectrode, semi-infinite diffusion results in peak-shaped voltammetric profiles, while microelectrodes, due to their size, convergent diffusion produces a steady-state limiting current [42], where the current can be described by:

$$I_L = 4nFDCr \quad (13)$$

where  $n$  is the number of electrons participating in the electron transfer process,  $F$  is the Faraday constant,  $D$  is the diffusion coefficient,  $C$  is the concentration of the electro-active species,  $r$  is the radius of a single microelectrode on the array. The benefits of utilizing such an electrode design include: enhanced mass transport due to the small diffusion layer across the surface and the convergent diffusion at its edges, allowing steady state limiting currents to be achieved; increased current densities; decrease in both ohmic drop and lower capacitance which increases the signal-to-background ratio and improves the response time of the system. That said, a drawback is the low absolute current output, with the measured currents often in the nano to sub-nanoampere range and the current measurement sensitive to issues of electrical noise, often necessitating the use of a Faraday cage/electrical shielding; such a requirement can negatively impact their applications in real world sensing devices. To overcome these issues and utilize the beneficial properties of a microelectrode, a microelectrode array is often utilized. In this configuration, the electrode surface is comprised of many microelectrodes, and if the electrode surface is designed correctly, with no overlap of diffusional layers between neighbouring microelectrodes, Eq. (13) becomes:

$$I_L = 4nFDCrN \quad (14)$$

where  $N$  is the total number of microelectrodes comprising the array. In this electrode configuration, the current output is effectively multiplied by the number of microelectrodes making up the array which clearly shows that the signal is amplified, overcoming issues identified above. Lawrence et al. [44] built upon the advantages of BDD and microelectrode arrays by developing and utilizing a BDD-array, which was shown to usefully measure manganese via cathodic stripping voltammetry. The BDD-array is in a hexagonal pattern, with 14 microelectrodes each having a 15  $\mu\text{m}$  diameter, which was micro-machined to prepare and coat a patterned BDD substrate with an intrinsic diamond insulating layer and has the advantage of the array being co-planar to the dielectric surroundings. The BDD-array is advantageous since the electrode is planar and made entirely of diamond, removing the problem of 'sealing' the microelectrodes in their insulating material as experienced with the earlier BDD-arrays. The BDD-array demonstrated the measurement of manganese (II) with a linear range from 1.8 to 9.2  $\mu\text{M}$  using a 120 s deposition time with a LOD of 49 nM.

Following the theme of forced convection, Gibbon-Walsh [45]

utilized a vibrating gold microwire electrode (10  $\mu\text{m} \times 0.5 \text{ mm}$ ) alongside anodic stripping chronopotentiometry to measure manganese (II) and zinc (II) in seawater. The use of vibration reduces the diffusion layer to around one micron [45], greatly improving mass transport and results in a lower detection limit. Other work using chronopotentiometry has specifically utilized derivative anodic stripping chronopotentiometry (dASCP) upon a mercury electrode for the trace manganese determination in different fresh vegetables and aromatic plants [46].

Banks et al. [47] compared three different electroanalytical sensing platforms for the detection of manganese (II); namely, the anodic stripping of manganese at an *in-situ* bismuth-film-modified boron-doped diamond electrode, CSV at a carbon paste electrode and CSV at a bare boron-doped diamond electrode. The first two methods were found to lack the required sensitivity and reproducibility whereas cathodic stripping voltammetry at a bare boron-doped diamond electrode is shown to be reliable and selective with a limit of detection, from applying a 60 s accumulation period, of  $7.4 \times 10^{-7} \text{ M}$ . The electroanalytical method was applied to determine manganese (II) in marine sediments which agreed with independent AAS. Other work has utilized edge plane pyrolytic graphite [48,49] comparing an edge plane pyrolytic graphite electrode with a BDD electrode, where it was found that in quiescent condition, the former is observed to have a three times high sensitivity; the method exhibited a linear range of 25 to 250 nM with an LOD of 14.2 nM and was validated in a certified seawater sample (NASS-5) from the National Research Council Canada [48]. Related to the sensing of manganese (II) in marine sediment, one interesting approach has utilized abrasive stripping voltammetry, where the manganese (II) containing sample, in this case microparticles of marine sediment containing manganese, is abrasively / mechanically transferred to a graphite electrode, which is then immersed into a suitable electrolyte to perform its qualitative determination [50].

Associated to the electrochemical sensing of manganese (II), potentiometric sensors have been developed for the measurement of manganese (II) offering benefits of good selectivity, sensitivity, precision, convenience and simplicity [51–60]. Potentiometric sensors are clearly able to measure down to the low nM range with wide linear ranges and response time from 10–40 s, depending on each sensor. Of note, Sahani and co-workers [51] developed a potentiometric sensor based upon an ionophore coated pyrolytic graphite electrode with a linear sensing range of  $1.23 \times 10^{-8}$  to  $1.0 \times 10^{-1} \text{ mol L}^{-1}$  and a LOD of  $4.78 \times 10^{-9} \text{ M}$  with a Nernstian slope of  $29.5 \pm 0.4 \text{ mV decade}^{-1}$  of activity. The sensor performs over a wide pH range of 3.5 to 9.0 and exhibited a quick response time of 9 s. The authors successfully demonstrated their potentiometric sensor to measure manganese in wastewater, soil and vegetables and validated the sensor against independent AAS. What is clear, is that the majority of potentiometric sensors are not validated in real samples nor with independent AAS for example, as such this is clearly an area to focus upon.

Joca and co-workers [25] have used gold electrodes with square-wave cathodic stripping voltammetry to determine manganese (II) in cement and clinker samples using an ultrasonic-assisted digestion protocol. The extraction of manganese by ultrasonic extraction involves taking 1.0 g of the cement or clinker samples, transferring to a polypropylene flask and treating with 20 mL of 3 M HCL, before being placed into an ultrasonic bath for 20 min. The authors compared the result obtained by flame atomic absorption spectrometry against traditionally utilized hot plate extraction, which involves the same reagents but requires boiling the sample for 15 min. It was demonstrated that the ultrasonic-assisted extraction gives identical results to the hot plate method, but noting that ultrasonic-assisted extraction is advantageous as it is much simpler and safer. Joca and co-workers demonstrated their electroanalytical protocol gave rise to a LOD of  $3.1 \times 10^{-8} \text{ M}$  using a 180 s deposition time and demonstrated the electroanalytical method to be consistent with independent flame atomic absorption spectrometry in the measurement of manganese in their chosen real samples [25].

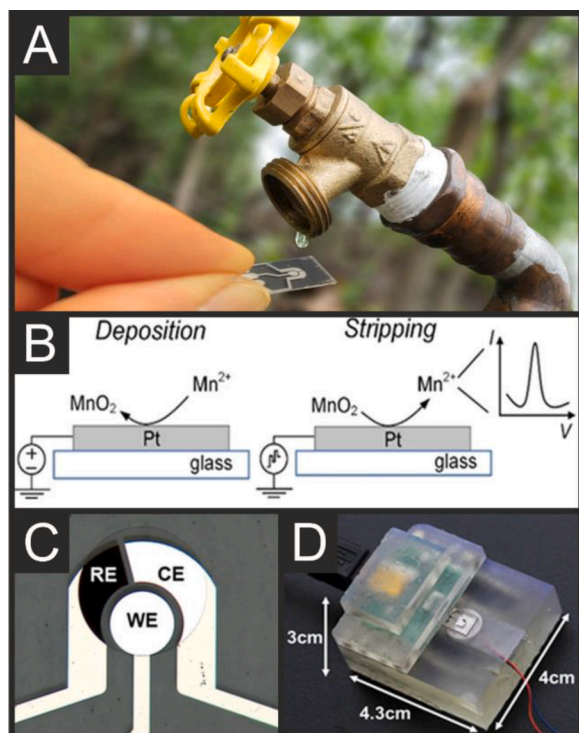


**Fig. 2.** (A) Overview of the sensing of manganese in drinking water using a thin-film Pt electrodes for the determination of Mn. (B) Schematic of the detection principle of CSV, illustrating the deposition phase to oxidize  $\text{Mn}^{2+}$  into  $\text{Mn}^{4+}$ , which forms a layer of  $\text{MnO}_2$  on the surface of the Pt WE, and the stripping phase to reduce  $\text{Mn}^{4+}$  back to  $\text{Mn}^{2+}$  off the electrode. (C) Photograph of the three-electrode microfabricated sensor with a 1 mm diameter circular Pt WE, a Pt CE, and an Ag/AgCl RE (WE = working electrode, RE = reference electrode, CE = counter electrode). (D) Three-dimensional (3-D)-printed interface housing the sensor, micro-vibration motor, and the mini-USB connection to the potentiostat. Reprinted with permission from Ref. [63]. Copyright (2021) American Chemical Society.

Screen-printed shallow recessed electrodes [61] and recessed microelectrodes arrays [62] have been reported. Microelectrode fabrication typically uses photolithography and sealing wires within glass, while in contrast, the screen-printing of microelectrodes has the advantage of reproducibility, simplicity and the ability to produce en-mass at a low production cost. Kadara and co-workers [62] reported the fabrication of recessed microelectrode arrays arranged in a hexagonal arrangement with one array comprising 16 microdiscs which have the nearest neighbour (centre-to-centre) separation of  $1250\ \mu\text{m}$  and a second array comprising 6 microdiscs with a separation of  $2500\ \mu\text{m}$ ; both were compared and contrasted. The array with the largest inter-electrode separation was found to give better analytical results due to the diffusional independence of each microelectrode with a linear range 90 to  $1780\ \text{nM}$  with a LOD of  $64\ \text{nM}$ , using a 30 s deposition time for the sensing of manganese (II).

Related to SPEs, in terms of portability, miniature platinum electrodes have been reported. Building on their previous work, [26,27] Boselli et al. [63] have utilized commercially available platinum thin-film electrodes, see Fig. 2, where the platinum film has been deposited onto a glass substrate. The electrode is housed within a 3D printed interface, where a micro-vibration motor vibrating at 12,000 rpm was utilized during the accumulation step. Using a 900 s deposition time, the authors demonstrated that the sensor could measure manganese with a LOD of  $10.1\ \text{nM}$ . The sensor was validated with drinking water samples ( $n = 78$ ) showing 100% agreement,  $\sim 70\%$  accuracy, and 91% precision when compared with ICP-MS. These results suggest that an electrochemical sensor based on Pt can be a useful and convenient

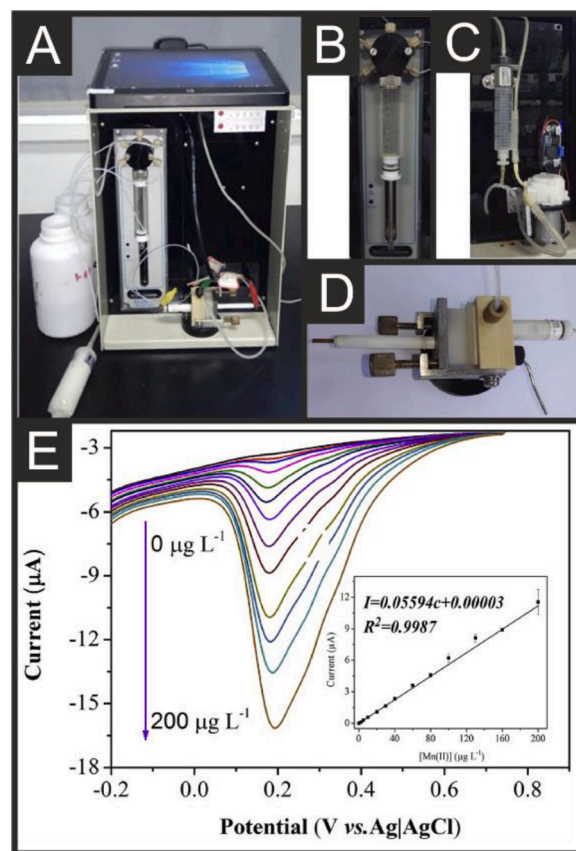


**Fig. 3.** (A) The sequential injection analysis device (the solution container and a peristaltic pump are hidden within the apparatus). (B) The syringe pump and the multi-position selection valve. (C) The solution container and the peristaltic pump. (D) An electrochemical flow cell. (E) Cathodic stripping voltammetric curves of the different concentration of Mn(II) from 0 to  $200\ \mu\text{g L}^{-1}$  and the corresponding calibration curve, inset. Reprinted with permission from Ref. [32]. Copyright (2020) Elsevier.

component of a sensing system for the rapid determination of manganese in drinking water at the point-of-use.

Mc Eleney et al. [64] developed an automated electrochemical flow cell, as shown in Fig. 3, replacing the traditional three-electrode model. In this bespoke device, the syringe pump and the multi-position selection valve are directly connected, and a solution container is also used to improve the reproducibility. The size of the device is  $25\ \text{cm} \times 23\ \text{cm} \times 37\ \text{cm}$  (length  $\times$  width  $\times$  height) and the weight of this device is 9.1 kg. Using sequential injection analysis, the LOD is found to be  $0.63\ \mu\text{g L}^{-1}$ , with a linear range from  $2.5$  to  $200\ \mu\text{g L}^{-1}$ ; Fig. 3 shows the observed cathodic stripping voltammetric peaks and corresponding calibration plot. The device was shown to successfully measure manganese in tap and lake water agreeing well with independent ICP-MS.

Recently, Additive manufacturing is emerging as a promising technology for the rapid and economical fabrication of portable electroanalytical devices [65,66]. Rocha and co-workers [65] additively manufactured electrochemical sensing platforms for manganese (II) determination. Despite the electrode comprising only 25 wt% nano-graphite and 75 wt% plastic (polylactic acid), a linear range from  $9.1 \times 10^{-9}\ \text{M}$  to  $2.7 \times 10^{-6}\ \text{M}$  is possible with a LOD of  $1.6 \times 10^{-9}\ \text{M}$ . The proposed electroanalytical method was successfully applied to the determination of manganese (II) in tap water samples and in the analysis of a certified material (drinking water). Such an approach holds promise for in-loco analyzes due to the portability of sensing and the use of AM-printed electrodes is attractive due to their low cost and versatility; for example it has recently been shown that a fully additively manufactured electrochemical cell printed *all-in-one* is possible, where all the

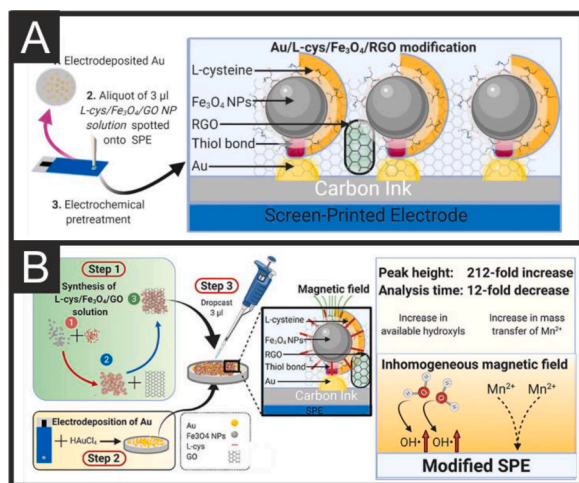


**Fig. 4.** (A) Graphical illustration of the electrode surface modification process and post-modified SPE. (B) An overview of how the electrode is produced, its structure, operating mechanism and its analytical performance. Reprinted with permission from Ref. [64]. Copyright (2021) Elsevier.

electrodes and cell are printed as one, requiring no post-assembly or external electrodes and it should be feasible to do the same for manganese determination [67].

Last, a novel magneto-electrochemical sensing methodology has been developed, see Fig. 4 [64]. Magnetic fields applied to an electrode surface are well known to increase the rate of mass transfer, which is dependant upon the nature of ion - whether it is para- or dia- magnetic. Mc Eleney and co-workers [64] have developed an electrodeposited nanogold modified screen-printed electrode, then modified via drop-casting with Fe<sub>3</sub>O<sub>4</sub> nanoparticles (<50 nm) functionalised with L-cysteine within a reduced graphene oxide matrix for the determination of manganese (II); the gold nanoparticles provide a self-assembly point for the functionalised Fe<sub>3</sub>O<sub>4</sub> nanoparticles via the thiol group present on the L-cysteine residue. The authors report that the magnetic Fe<sub>3</sub>O<sub>4</sub> nanoparticles significantly increased the diffusion coefficient of the paramagnetic Mn<sup>2+</sup> ion during the electrodeposition step and additionally increased the number of hydroxyls available for the formation of the MnO<sub>2</sub> layer, attributed to chiral induced spin selectivity. The reduced graphene oxide (rGO) also serves to increase the surface area and heterogenous electron transfer rate of the intermediate reactions. The composite electrodes, using SW-CSV, was shown to detect Mn<sup>2+</sup> from 0.5 to 300 μg L<sup>-1</sup> and 62 to 1500 μg L<sup>-1</sup> using deposition times of 300 or 30 s, respectively. Using this magneto-electrochemical sensing methodology and composite electrode, a significant enhancement of the Mn<sup>2+</sup> response signal, a 212-fold increase compared to a bare SPE was observed. The authors determined manganese (II) in ten soil sample extracts and showed good agreement with FAAS.

## 1.2. Summary and outlook

In summary it is evident that the electroanalytical determination of manganese (II) is possible with high sensitivity and selectivity, comparable to laboratory instrumentation yet having the advantage of being portable and low cost. It is noted that CSV is the prominent electroanalytical technique used for the determination of manganese (II), providing clear advantages over ASV. We can observe that the electroanalytical sensing of manganese (II) in water samples is a major area of reported research at levels that will be found in-the-field, with of-course higher concentrations measurable following suitable dilution. These are also independently validated against laboratory equipment instrumentation providing evidence that those electroanalytical based sensors can potentially be implanted into the field for the routine sensing of manganese (II). However, one area that needs attention is the area of

manganese (II) determination in food. We know that manganese (II) is ingested from drinking water and food sources, yet the amount of academic literature exploring the latter is sparse; this is an area to focus upon. Last, potentiometric sensors are reported but few, if any, are validated against standard laboratory instrumentation and worse still, very few, if any, real samples have been reported, questioning its use for manganese (II) determination.

## Declaration of Competing Interest

The authors declare that they have no known competing financial interests or personal relationships that could have appeared to influence the work reported in this paper.

## References

- [1] B. Furbee, M.R. Dobbs, CHAPTER 26 - manganese. *Clinical Neurotoxicology*, W.B. Saunders, Philadelphia, 2009, pp. 293–301.
- [2] P. Grandjean, P.J. Landrigan, Neurobehavioural effects of developmental toxicity, *Lancet Neurol.* 13 (2014) 330–338.
- [3] M.A. Rahman, M.A. Hashem, M.S. Rana, M.R. Islam, Manganese in potable water of nine districts, Bangladesh: human health risk, *Environ. Sci. Pollut. Res.* 28 (2021) 45663–45675.
- [4] S.H. Frisbie, E.J. Mitchell, H. Dustin, D.M. Maynard, B. Sarkar, World Health Organization discontinues its drinking-water guideline for manganese, *Environ. Health Perspect.* 120 (2012) 775–778.
- [5] F.J. Feldman, R.E. Bosshart, G.D. Christian, Sensitivity of manganese determination by atomic absorption spectrometry using four solvents, *Anal. Chem.* 39 (1967) 1175–1177.
- [6] K.C. Teo, J. Chen, Determination of manganese in water samples by flame atomic absorption spectrometry after cloud point extraction, *Analyst* 126 (2001) 534–537.
- [7] V.L. Biddle, E.L. Wehry, Fluorometric determination of manganese(II) via catalyzed enzymic oxidation of 2,3-diketogulonate, *Anal. Chem.* 50 (1978) 867–870.
- [8] R.M. Lattuada, C.T.B. Menezes, P.T. Pavei, M.C.R. Peralba, J.H.Z. Dos Santos, Determination of metals by total reflection X-ray fluorescence and evaluation of toxicity of a river impacted by coal mining in the south of Brazil, *J. Hazard. Mater.* 163 (2009) 531–537.
- [9] E.J. Daftsis, G.A. Zachariadis, Analytical performance of a multi-element ICP-AES method for Cd, Co, Cr, Cu, Mn, Ni and Pb determination in blood fraction samples, *Microchim. Acta* 160 (2008) 405–411.
- [10] K. Sreenivasa Rao, T. Balaji, T. Prasada Rao, Y. Babu, G.R.K. Naidu, Determination of iron, cobalt, nickel, manganese, zinc, copper, cadmium and lead in human hair by inductively coupled plasma-atomic emission spectrometry, *Spectrochim. Acta Part B* 57 (2002) 1333–1338.
- [11] A.G.M. Ferrari, S.J. Rowley-Neale, C.E. Banks, Screen-printed electrodes: transitioning the laboratory in-to-the field, *Talanta Open* 3 (2021), 100032.
- [12] R.J. O'Halloran, Anodic stripping voltammetry of manganese in seawater at a mercury film electrode, *Anal. Chim. Acta* 140 (1982) 51–58.
- [13] T.M. Florence, Comparison of linear scan and differential pulse anodic stripping voltammetry at a thin mercury film glassy carbon electrode, *Anal. Chim. Acta* 119 (1980) 217–223.
- [14] A. Kumar, M. Kataly, B.K. Puri, Polarographic behaviour of zinc(II) and manganese (II) at a dropping-mercury electrode using δ-valerolactam as a complexing agent, *Analyst* 112 (1987) 979–981.
- [15] V. Stara, M. Kopanica, Determination of manganese using the method of electrochemical enrichment, *Electroanalysis* 5 (1993) 595–598.
- [16] Z.Rady Komy, DPASV method for determination of trace concentrations of manganese in non-buffered chloride solutions by addition of cyanide as a masking agent, *Microchim. Acta* 135 (2000) 35–43.
- [17] R. Piech, B. Baś, W.W. Kubiak, The cyclic renewable mercury film silver based electrode for determination of manganese(II) traces using anodic stripping voltammetry, *J. Electroanal. Chem.* 621 (2008) 43–48.
- [18] O.M.S. Filipe, C.M.A. Brett, Cathodic stripping voltammetry of trace Mn(II) at carbon film electrodes, *Talanta* 61 (2003) 643–650.
- [19] L. Lesven, S.M. Skogvold, Ø. Mikkelsen, G. Billon, Determination of manganese in natural media by anodic stripping voltammetry using a rotating solid silver amalgam electrode, *Electroanalysis* 21 (2009) 274–279.
- [20] W. Yue, A. Bange, B.L. Riehl, B.D. Riehl, J.M. Johnson, I. Papautsky, et al., Manganese detection with a metal catalyst free carbon nanotube electrode: anodic versus cathodic stripping voltammetry, *Electroanalysis* 24 (2012) 1909–1914.
- [21] C.E. Banks, A. Crossley, C. Salter, S.J. Wilkins, R.G. Compton, Carbon nanotubes contain metal impurities which are responsible for the “Electrocatalysis” seen at some nanotube-modified electrodes, *Angew. Chem. Int. Ed.* 45 (2006) 2533–2537.
- [22] K. Jurkschat, X. Ji, A. Crossley, R.G. Compton, C.E. Banks, Super-washing does not leave single walled carbon nanotubes iron-free, *Analyst* 132 (2007) 21–23.
- [23] S. Rodrigues, A.K. Shukla, N. Munichandraiah, A cyclic voltammetric study of the kinetics and mechanism of electrodeposition of manganese dioxide, *J. Appl. Electrochem.* 28 (1998) 1235–1241.
- [24] S. Nijjer, J. Thonstad, G.M. Haarberg, Oxidation of manganese(II) and reduction of manganese dioxide in sulphuric acid, *Electrochim. Acta* 46 (2000) 395–399.



- [25] J.F.S. Joca, F.S. Felix, L. Angnes, Ultrasonic-assisted digestion of cement and clinker samples for the determination of manganese by square wave cathodic stripping voltammetry, *Anal. Lett.* 53 (2020) 1075–1086.
- [26] W. Kang, X. Pei, A. Bange, E.N. Haynes, W.R. Heineman, I. Papautsky, Copper-based electrochemical sensor with palladium electrode for cathodic stripping voltammetry of manganese, *Anal. Chem.* 86 (2014) 12070–12077.
- [27] W. Kang, C. Rusinek, A. Bange, E. Haynes, W.R. Heineman, I. Papautsky, Determination of manganese by cathodic stripping voltammetry on a microfabricated platinum thin-film electrode, *Electroanalysis* 29 (2017) 686–695.
- [28] E.A. Viltchinskaia, L.L. Zeigman, D.M. Garcia, P.F. Santos, The effect of organic substances and electrochemical elimination of it for cathodic stripping voltammetric determination of manganese (II) in natural waters, *Anal. Lett.* 28 (1995) 1845–1863.
- [29] J. Labuda, M. Vaníčková, E. Beinrohr, Determination of dissolved manganese in natural waters by differential pulse cathodic stripping voltammetry, *Microchim. Acta* 97 (1989) 113–120.
- [30] J. Di, F. Zhang, Voltammetry determination of trace manganese with pretreatment glassy carbon electrode by linear sweep voltammetry, *Talanta* 60 (2003) 31–36.
- [31] N. Abo El-Maali, D. Abd El-Hady, Square-wave adsorptive stripping voltammetry at glassy carbon electrode for selective determination of manganese. Application to some industrial samples, *Anal. Chim. Acta* 370 (1998) 239–249.
- [32] Z. Lai, F. Lin, L. Qiu, Y. Wang, X. Chen, H. Hu, Development of a sequential injection analysis device and its application for the determination of Mn(II) in water, *Talanta* 211 (2020), 120752.
- [33] N.Y. Stozhko, O.V. Inzhevatova, L.L. Kolyadina, G.N. Lipunova, A thick-film graphite-containing electrode modified with formazan for determining manganese in natural and drinking waters by stripping voltammetry, *J. Anal. Chem.* 60 (2005) 163–168.
- [34] Y. Pei, J.F. McLeod, S.J. Payne, Z. She, A comparative study of electroanalytical methods for detecting manganese in drinking water distribution systems, *Electrocatalysis* 12 (2021) 176–187.
- [35] J. Zhou, R. Neeb, Contribution to the adsorption voltammetric determination of manganese, *Fresenius J. Anal. Chem.* 350 (1994) 593–598.
- [36] S.B. Khoo, M.K. Soh, Q. Cai, M.R. Khan, S.X. Guo, Differential pulse cathodic stripping voltammetric determination of manganese(II) and manganese(VII) at the 1-(2-pyridylazo)-2-naphthol-modified carbon paste electrode, *Electroanalysis* 9 (1997) 45–51.
- [37] A. Romanus, H. Müller, D. Kirsch, Application of adsorptive stripping voltammetry (AdSV) for the analysis of trace metals in brine, *Fresenius J. Anal. Chem.* 340 (1991) 363–370.
- [38] S.E.W. Jones, R.G. Compton, Stripping analysis using boron-doped diamond electrodes, *Curr. Anal. Chem.* 4 (2008) 170–176.
- [39] A.J. Saterlay, J.S. Foord, R.G. Compton, Sono-cathodic stripping voltammetry of manganese at a polished boron-doped diamond electrode: application to the determination of manganese in instant tea, *Analyst* 124 (1999) 1791–1796.
- [40] C.E. Banks, R.G. Compton, A.C. Fisher, I.E. Henley, The transport limited currents at insonated electrodes, *Phys. Chem. Chem. Phys.* 6 (2004) 3147–3152.
- [41] C.E. Banks, R.G. Compton, Ultrasonically enhanced voltammetric analysis and applications: an overview, *Electroanalysis* 15 (2003) 329–346.
- [42] R.G. Compton, C.E. Banks, *Understanding Voltammetry*, World Scientific, 2018.
- [43] J.-Y. Jin, F. Xu, T. Miwa, Square-wave cathodic stripping voltammetry of ultratrace manganese in the presence of ultrasound irradiation, *Anal. Sci.* 16 (2000) 317–319.
- [44] N.S. Lawrence, M. Pagels, A. Meredith, T.G.J. Jones, C.E. Hall, C.S.J. Pickles, et al., Electroanalytical applications of boron-doped diamond microelectrode arrays, *Talanta* 69 (2006) 829–834.
- [45] K. Gibbon-Walsh, P. Salatin, C.M.G. van den Berg, Determination of manganese and zinc in coastal waters by anodic stripping voltammetry with a vibrating gold microelectrode, *Environ. Chem.* 8 (2011) 475–484.
- [46] G. Dugo, L. La Pera, V.L. Turco, R.M. Palmieri, M. Saitta, Effect of boiling and peeling on manganese content of some vegetables determined by derivative anodic stripping chronopotentiometry (dASCP), *Food Chem.* 93 (2005) 703–711.
- [47] C.E. Banks, J. Kruusma, R.R. Moore, P. Tomčík, J. Peters, J. Davis, et al., Manganese detection in marine sediments: anodic vs. cathodic stripping voltammetry, *Talanta* 65 (2005) 423–429.
- [48] Christine M. Welch, Craig E. Banks, Šebojka Komorsky-Lovrić, Richard G. Compton, Electroanalysis of trace manganese via cathodic stripping voltammetry: exploration of edge plane pyrolytic graphite electrodes for environmental analysis *Croat. Chem. Acta*, 79(2006) 27–32.
- [49] F. Wantz, C.E. Banks, R.G. Compton, Edge plane pyrolytic graphite electrodes for stripping voltammetry: a comparison with other carbon based electrodes, *Electroanalysis* 17 (2005) 655–661.
- [50] S. Komorsky-Lovric, A simple method, *Croat. Chem. Acta* 2 (1998) 263–269.
- [51] M.K. Sahani, A.K. Singh, A.K. Jain, Nano-level monitoring of Mn<sup>2+</sup> ion by fabrication of coated pyrolytic graphite electrode based on isonicotinohydrazide derivatives, *Mater. Sci. Eng. C* 50 (2015) 124–132.
- [52] M. Junko, N. Hiroshi, I. Sanae, T. Nobuyuki, The preparation and properties of the manganese(II) ion-selective electrode, *Bull. Chem. Soc. Jpn.* 59 (1986) 39–42.
- [53] A.K. Singh, P. Saxena, A. Panwar, Manganese(II)-selective PVC membrane electrode based on a pentaazamacrocyclic manganese complex, *Sens. Actuators B* 110 (2005) 377–381.
- [54] V.K. Gupta, A.K. Jain, G. Maheshwari, Manganese (II) selective PVC based membrane sensor using a Schiff base, *Talanta* 72 (2007) 49–53.
- [55] M. Aghaie, M. Giah, M. Zawari, Manganese(II) ion-selective membrane electrode based on N-(2-picolinamido ethyl)-picolinamide as neutral carrier, *Bull. Korean Chem. Soc.* 31 (2010) 2980–2984.
- [56] M.H. Mashhadizadeh, E.P. Taheri, I. Sheikhsaie, A novel Mn<sup>2+</sup> PVC membrane electrode based on a recently synthesized Schiff base, *Talanta* 72 (2007) 1088–1092.
- [57] A.A. Khan, A. Khan, U. Habiba, L. Paquiza, S. Ali, Preparation and characterization of electrically conducting polypyrrole Sn(IV) phosphate cation-exchanger and its application as Mn(II) ion selective membrane electrode, *J. Adv. Res.* 2 (2011) 341–349.
- [58] I. Sheikhsaie, T. Shamspur, S.Y. Ebrahimipur, Asymmetric Schiff base as carrier in PVC membrane electrodes for manganese (II) ions, *Arab. J. Chem.* 5 (2012) 201–205.
- [59] A.K. Singh, K.R. Bandi, A. Upadhyay, A.K. Jain, A comparative study on fabrication of Mn<sup>2+</sup> selective polymeric membrane electrode and coated graphite electrode, *Mater. Sci. Eng. C* 33 (2013) 626–633.
- [60] T.A. Ali, G.G. Mohamed, Determination of Mn(II) ion by a modified carbon paste electrode based on multi-walled carbon nanotubes (MWCNTs) in different water samples, *Sens. Actuators B* 202 (2014) 699–707.
- [61] J.P. Metters, F. Tan, R.O. Kadara, C.E. Banks, Electroanalytical properties of screen printed shallow recessed electrodes, *Anal. Methods* 4 (2012) 3140–3149.
- [62] R.O. Kadara, N. Jenkinson, C.E. Banks, Screen printed recessed microelectrode arrays, *Sens. Actuators B* 142 (2009) 342–346.
- [63] E. Boselli, Z. Wu, A. Friedman, B. Claus Henn, I. Papautsky, Validation of electrochemical sensor for determination of manganese in drinking water, *Environ. Sci. Technol.* 55 (2021) 7501–7509.
- [64] C. Mc Eleney, S. Alves, D. Mc Crudden, Novel magneto-electrochemical determination of Mn(II), *J. Electroanal. Chem.* 900 (2021), 115734.
- [65] D.P. Rocha, C.W. Foster, R.A.A. Munoz, G.A. Buller, E.M. Keefe, C.E. Banks, Trace manganese detection via differential pulse cathodic stripping voltammetry using disposable electrodes: additively manufactured nanographite electrochemical sensing platforms, *Analyst* 145 (2020) 3424–3430.
- [66] K.R. Ryan, M.P. Down, C.E. Banks, Future of additive manufacturing: overview of 4D and 3D printed smart and advanced materials and their applications, *Chem. Eng. J.* 403 (2021), 126162.
- [67] R.D. Crapnell, E. Bernalte, A.G.-M. Ferrari, M.J. Whittingham, R.J. Williams, N. J. Hurst, et al., All-in-one single-print additively manufactured electroanalytical sensing platforms, *ACS Meas. Sci.* 2 (2) (2022) 167–176.
- [68] J.S. Roitz, K.W. Bruland, Determination of dissolved manganese(II) in coastal and estuarine waters by differential pulse cathodic stripping voltammetry, *Anal. Chim. Acta* 344 (1997) 175–180.
- [69] C. Locatelli, G. Torsi, Determination of Se, As, Cu, Pb, Cd, Zn and Mn by anodic and cathodic stripping voltammetry in marine environmental matrices in the presence of reciprocal interference. Proposal of a new analytical procedure, *Microchem. J.* 65 (2000) 293–303.
- [70] J.-Y. Jin, F. Xu, T. Miwa, Cathodic stripping voltammetry for determination of trace manganese with graphite/styrene-acrylonitrile copolymer composite electrodes, *Electroanalysis* 12 (2000) 610–615.
- [71] A. Goodwin, A.L. Lawrence, C.E. Banks, F. Wantz, D. Omanović, Š. Komorsky-Lovrić, et al., On-site monitoring of trace levels of free manganese in sea water via sonoelectroanalysis using a boron-doped diamond electrode, *Anal. Chim. Acta* 533 (2005) 141–145.
- [72] B. Rezaei, M. Ghiaci, M.E. Sedaghat, A selective modified bentonite-porphyrin carbon paste electrode for determination of Mn(II) by using anodic stripping voltammetry, *Sens. Actuators B* 131 (2008) 439–447.